

We are IntechOpen, the world's leading publisher of Open Access books Built by scientists, for scientists

6,900

Open access books available

185,000

International authors and editors

200M

Downloads

Our authors are among the

154

Countries delivered to

TOP 1%

most cited scientists

12.2%

Contributors from top 500 universities



WEB OF SCIENCE™

Selection of our books indexed in the Book Citation Index
in Web of Science™ Core Collection (BKCI)

Interested in publishing with us?
Contact book.department@intechopen.com

Numbers displayed above are based on latest data collected.
For more information visit www.intechopen.com



Optoelectronic Plethysmography for Measuring Rib Cage Distortion

Giulia Innocenti Bruni¹, Francesco Gigliotti¹ and Giorgio Scano^{1,2}

¹*Fondazione Don Carlo Gnocchi, Pozzolatico Firenze*

²*Department of Internal Medicine,
Section of Clinical Immunology and Respiratory Medicine
Italy*

1. Introduction

The pressure acting on the part of the Rib Cage that is apposed to the costal surface of the lung is quite different from that acting on the part apposed to the diaphragm. The non uniformity of pressure distribution led Agostoni and D'Angelo (1985) to suggest that the rib cage could be usefully regarded as consisting of two compartments mechanically coupled to each other (Agostoni & D'Angelo, 1985; Jiang et al., 1988, Ward, 1992): the pulmonary rib cage (RCp), and the abdominal rib cage (RCa). The magnitude of the coupling determines the resistance to distortion and is an important parameter in the mechanics of breathing. Unitary behaviour of the rib cage was thought to be dictated by rigidity and the restrictive nature of rib articulations and interconnection. Nonetheless, important distortion of the rib cage from its relaxation configuration has been described in asthma (Ringel et al., 1983) quadriplegia (Urmey et al., 1981) and also in healthy individual during a variety of breathing pattern (quiet breathing, hyperventilation, single inspiration, involuntary breathing acts, such as phrenic nerve stimulation); (Crawford et al., 1983; McCool et al., 1985; Ward et al., 1992; D'Angelo, 1981; Roussos et al., 1977). In summarizing these results Crawford et al., (1983) and more recently McCool et al., (1985) concluded that the maintenance of rib cage shape needs not be attributed to inherent stiffness but may be the consequence of apparently coordinated activity of the different respiratory muscles. Under circumstance such as lung hyperinflation or when mechanical coupling between the upper rib cage (RCp) and the lower rib cage (RCa) is very loose rib cage muscle recruitment is essential to prevent paradoxical (inward) rib cage displacement. (Ward et al., 1992). Moreover the deformation of the chest wall (CW) occurring during hyperventilation and while breathing through a resistance implies that the work of breathing in these conditions is slight larger than that calculated only the basis of the volume-pressure diagram. And indeed part of the force exerted by the respiratory muscles is expended to change the shape of the chest wall relative to that occurring at the same lung volume during relaxation (Agostoni & Mognoni 1966).

Most of what is known about the kinematics of the chest wall i.e., the thoraco-abdomen compartment comes from studies (Sackner, 1980; Gilbert et al., 1972) using RIP (Respirace®). However, the RIP method is subject to error, the volume being inferred from cross-sectional area changes. Also, evaluation of the breathing pattern with RIP is reliable only when the rib cage and abdomen behave with a single degree of freedom such as during

quiet breathing. The validity of the calibration coefficient obtained experimentally to convert one or two dimensions to volume is limited to the estimation of tidal volume under conditions matched with those during which the calibration was performed (Henke et al., 1988). Conversely, OEP has been proven able to evaluate, without any assumptions regarding degree of freedom, changes in compartmental volume of the chest wall. (Pedotti et al., 1995; Cala et al., 1996; Kenyon et al., 1997; Sanna et al., 1999; Aliverti et al., 1997; Duranti et al., 2004; Romagnoli et al., 2004a; Romagnoli et al., 2004b; Romagnoli et al., 2006; Binazzi et al., 2006; Filippelli et al., 2001; Lanini et al., 2007; Gorini et al., 1999; Filippelli et al., 2003). The precise assessment of changes in thoraco-abdominal volumes, combined with pressure measurements, allows a detailed description of the action and control of the different respiratory muscle groups. That is the reason why the accurate computation of thoraco-abdominal volume changes is needed. It is well known that methods actually in use for the computation of thoraco-abdominal volume displacement are affected by several limitations. The most used devices able to compute dynamic changes of the thoraco-abdominal wall are magnetometers and inductance plethysmography (Respirtrace®). Both these systems are based on the assumption that the thoraco-abdominal wall has only two degrees of freedom but it is well known that changes in both antero-posterior diameter and changes in cross-sectional area of thoracic and abdominal compartments are not linearly related to their respective volumes. Furthermore both devices are strongly influenced by artefacts due to the subject's posture that limit their utilization in dynamic conditions (e.g. exercise).

An ideal system able to measure movements and volumes of the respiratory system should have the following characteristics as much as possible:

1. Accurate computation of volume changes without using a mouthpiece that may alter the normal breathing pattern (Gilbert et al., 1972).
2. Necessitating of a simple, stable and repeatable calibration.
3. Possibility of use in non collaborating subjects (during sleep, or in unconscious patients).
4. Permitting the analysis in different postures.
5. Permitting the analysis in dynamic conditions such walking, or cycling.
6. Allowing high frequency response in order to accurately describe rapid phenomena (i.e. electric or magnetic stimulation of phrenic nerves).
7. Allowing the analysis of movements and volume changing of the different compartments of the chest wall: the upper thorax, lower thorax, and abdomen).
8. Allowing the analysis of movements and volume changing of the two halves (left and right) of the chest wall.
9. Being non-invasive, non-joining and safe for the patient.

An OEP device able to track the three-dimensional co-ordinates of a number of reflecting markers placed non-invasively on the skin of the subject satisfies many of these characteristics. The simultaneous acquisition of kinematic signals with pleural and gastric pressures during a relaxation manoeuvre allows the representation of pressure-volume plots describing the mechanical characteristics of each compartment. The OEP system was developed in 80's by the Bioengineering Department of the University of Milano in order to overcome as many of the previous limitations as possible (Pedotti et al., 1995; Cala et al., 1996; Kenyon et al., 1997)

Here we quantify distortion in healthy and diseased rib cage using a method that requires an accurate measurement of absolute volumes of upper and lower rib cage .

2. Methods

2.1 Subjects and experimental protocol

We studied non-smoking healthy subjects experienced in physiological studies and in performing respiratory manoeuvres, and patients with a number of respiratory disorders.

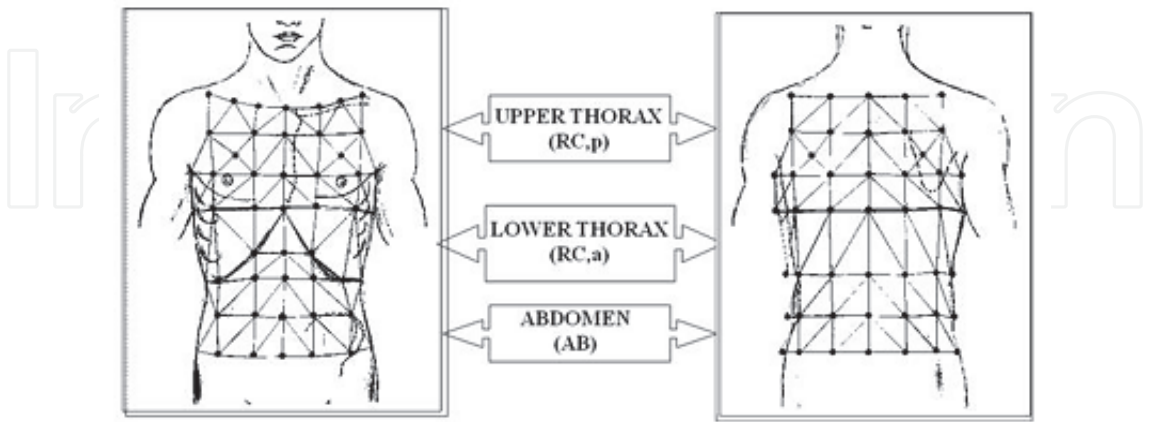


Fig. 1. Eighty-nine markers model.

Eighty-nine reflecting markers are placed in front and back over the trunk from the clavicles to the anterior superior iliac spines along predefined vertical and horizontal lines. To measure the Vcw compartments from the surface markers, we define the following: (i) the diaphragm border confirmed by percussion at end-expiration in sitting position, (ii) the boundaries of the upper rib cage (RCp) as extending from the clavicles to a line extending transversely around the thorax corresponding to the top of the area of the apposition of the diaphragm to the rib cage; (iii) the boundaries of lower rib cage (RCa) as extending from this line to the lower costal margin anteriorly, and to the level of the lowest point of the lower costal margin posteriorly, and (iv) the boundaries of the abdomen as extending caudally from the lower rib cage to a horizontal line at the level of the anterior superior iliac spine.

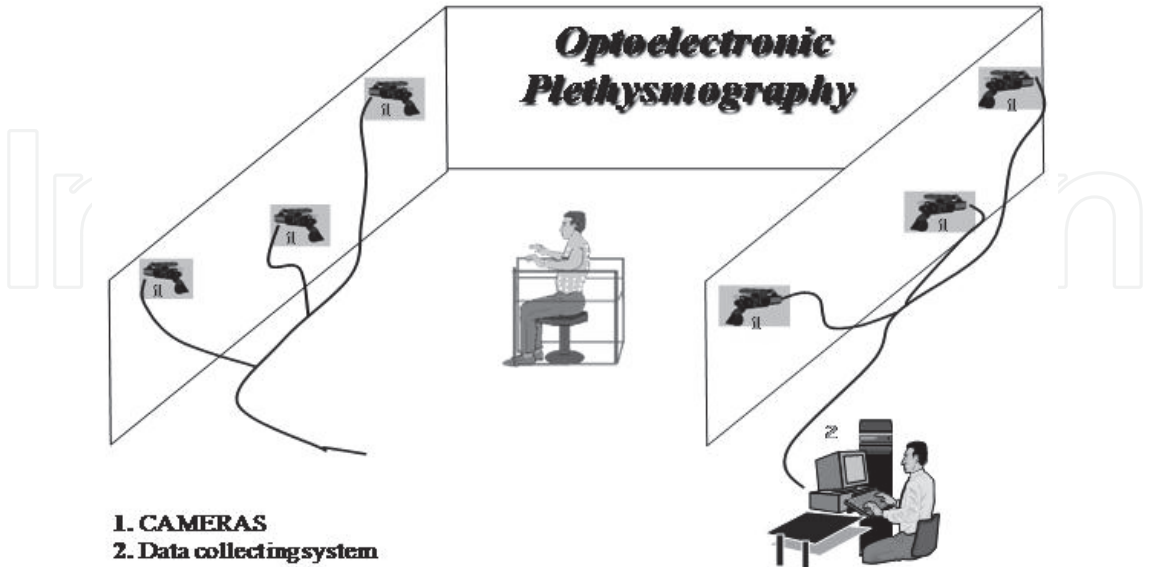


Fig. 2. The coordinates of the landmarks were measured with a system configuration of six infrared television cameras, three placed 4 m behind and three placed 4 m in front of the subject at a sampling rate of ≥ 60 Hz.

2.2 Compartmental volume measurements

Volumes of the different chest wall compartments were assessed by using the ELITE system, which allows computation of the 3-dimensional coordinates of 89 surface markers applied on the chest wall surface with high accuracy (Cala et al., 1996). The markers, small hemispheres (5 mm in diameter) coated with reflective paper, were placed circumferentially in seven horizontal rows between the clavicles and the anterior superior iliac spine. Along the horizontal rows, the markers were arranged anteriorly and posteriorly in five vertical columns, and there was an additional bilateral column in the mid-axillary line. In agreement with Cala et al., (1996), the anatomic landmarks for the horizontal rows were 1) the clavicular line, 2) the manubrio-sternal joint, 3) the nipples, 4) the xiphoid process, 5) the lower costal margin, 6) umbilicus, and 7) anterior superior iliac spine. The landmarks for the vertical rows were 1) the midlines, 2) both anterior and posterior axillary lines, 3) the midpoint of the interval between the midline and the anterior axillary lines, and 4) the midaxillary lines. To measure volume of chest wall (V_{cw}) compartments from the surface markers, we defined the following: (i) confirmed by percussion at end-expiration in sitting position, the diaphragm border in the mid clavicular line was always below the anterior end of the seventh rib, (ii) the boundaries of the upper rib cage (RC, p) as extending from the clavicles to a line extending transversely around the thorax corresponding to the top of the area of the apposition of the diaphragm to the rib cage, (iii) the boundaries of lower rib cage (RC, a) as extending from this line to the lower costal margin anteriorly, and to the level of the lowest point of the lower costal margin posteriorly, and (iv) the boundaries of the abdomen as extending caudally from the lower rib cage to a horizontal line at the level of the anterior superior iliac spine.

The coordinates of the landmarks were measured with a system configuration of six infrared television cameras, three placed 4 m behind and three placed 4 m in front of the subject at a sampling rate of 25-100 Hz. Starting from the marker coordinates, the thoraco-abdominal volumes were computed by triangulating the surface. For closure of surface triangulation, additional phantom markers were constructed as the average position of surrounding points at the center of the caudal and cephalad extremes of the trunk. Volumes were calculated from the surface triangulation between the marker points.

2.3 Pressure measurements

Pes and Pga were measured by using conventional balloon-catheter systems connected to two 100-cmH₂O differential pressure transducers (Validyne, Northridge, CA). Pes was used as an index of pleural pressure and Pga as that of abdominal pressure (Pab). From the pressure signals, we measured the following: Pes and Pga at end inspiration (PesEI and PgaEI, respectively) and end expiration (PesEE and PgaEE, respectively) at zero-flow points. The transdiaphragmatic pressure (Pdi) was obtained by subtracting Pes from Pga. Pdi at end expiration during quiet breathing was assumed to be zero. The difference between PgaEI and PesEI was defined as active Pdi and that between PgaEE and PesEE as passive Pdi. ΔP_{di} was defined as the difference between passive Pdi and active Pdi. Pressure and flow signals were synchronized to the kinematics signals of the OEP system and sent to an IBM-compatible personal computer through an RTI 800 analogue-to-digital card for subsequent analysis.

2.4 Rib cage and abdomen relaxation measurements

Relaxation characteristics of the chest wall were studied at rest. The subjects, in a sitting position, inhaled to total lung capacity and then relaxed and exhaled through a high

resistance. Relaxation manoeuvres were repeated until curves were reproducible, pressure at the mouth returned to zero at functional residual capacity (FRC), and Pdi was zero throughout the entire manoeuvre. The best relaxation curve was retained. To assess rib cage relaxation characteristics, volume of pulmonary rib cage ($V_{rc,p}$) was plotted against P_{es} . The best fitting linear ($y = ab + x$) regression for the $V_{rc,p}$ - P_{es} curve was constructed to obtain a relaxation curve of RC, p. The relaxation curve of the abdomen was obtained by plotting P_{ga} vs. V_{ab} from end-expiratory volume of abdomen (V_{ab}) to end-inspiratory V_{ab} during quiet breathing; we found a curvilinear relationship to which we fitted a second-order polynomial regression (Sanna et al., 1999; Aliverti et al., 1997). (This was extrapolated linearly from higher and lower values of V_{ab}). This method was preferred to the actual data obtained during relaxation because the latter were reliably obtained only at values of V_{ab} greater than at FRC.

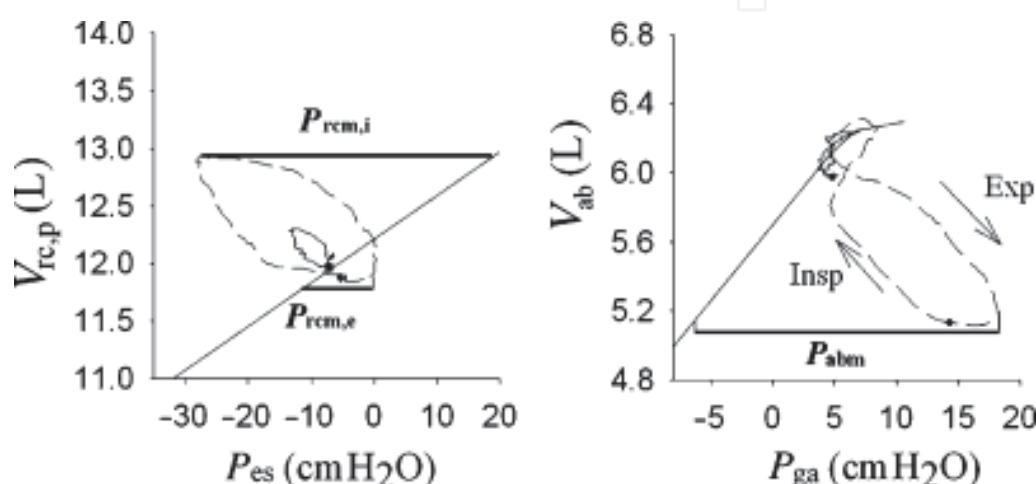


Fig. 3. Schematic representation of relationship between oesophageal pressure (P_{es}) and volume of pulmonary rib cage ($V_{rc,p}$) during quiet breathing (continuous loop) and at 50 L min^{-1} of VE (dashed loop) assuming minimal rib cage distortion during leg exercise. The thin line is the relaxation line. The closed circle is end expiratory volume. Measurement of pressure generated by rib cage muscles at $V_{rc,p}$ (thin line) is obtained from horizontal distance between dynamic loop and the relaxation line at that volume during inspiration ($P_{rcm,i}$) and expiration ($P_{rcm,e}$). Right: schematic representation of the relationship between gastric pressure (P_{ga}) and volume of the abdomen (V_{ab}) at rest and at 50 L min^{-1} of ventilation (VE). The thin line is the relaxation line. Measurement of pressure generated by abdominal muscles (P_{abm}) at that V_{ab} is obtained from the horizontal distance between gastric pressure and the relaxation line at that volume.

2.5 Cardiopulmonary exercise testing

Flow was measured with a mass flow sensor (Vmax 229; SensorMedics; 70 ml dead space) near the mouthpiece and lung volume changes were obtained by integrating the flow signal. A gas mixture (inspiratory oxygen fraction of 0.50 balanced with nitrogen) was inspired by the patients from a Douglas bag through a two-way non-rebreathing valve (mod 27900; Hans-Rudolph, Kansas City, MO, USA, 115 ml dead space). The flow into the Douglas bag was constant and patients breathed the gas mixture at the rate they demanded. We carefully reduced the impedance of the tubing by increasing its width and minimizing its length. To ascertain the linearity of the analyzer we used a 0.50 oxygen calibration cylinder. During the test flow rate at the mouth and gas exchange were recorded breath-by-breath (Vmax 229,

SensorsMedics). Expired gas was analyzed for oxygen uptake (V'_{O_2}), and carbon dioxide production (V'_{CO_2}). Cardiac frequency was continuously measured using a 12-lead electrocardiogram and oxygen saturation was measured using a pulse oxymeter (NPB 290; Nellcore Puritan Bennett, Pleasanton, CA, USA). The equipment was calibrated immediately before each test. V'_{CO_2} and V'_{O_2} were expressed as standard temperature, pressure and dry. The flow signal was synchronized to that of the motion analysis used for OEP and sent to a personal computer for subsequent analysis.

3. Analysis of the data

3.1 Operational chest wall volume measurements

To measure the Vcw compartments from the surface markers, we defined the following: (i) confirmed by percussion at end expiration in sitting position, the diaphragm border in the mid clavicular line was always below the anterior end of the seventh rib, (ii) the boundaries of the upper rib cage (RCp) as extending from the clavicles to a line extending transversely around the thorax corresponding to the top of the area of the apposition of the diaphragm to the rib cage; (iii) the boundaries of lower rib cage (RCa) as extending from this line to the lower costal margin anteriorly, and to the level of the lowest point of the lower costal margin posteriorly, and (iv) the boundaries of the abdomen as extending caudally from the lower rib cage to a horizontal line at the level of the anterior superior iliac spine. The arrangement of the chosen markers and the geometric model allow the computation of the contribution of rib cage and abdomen to tidal volume (VT). The difference between the end-inspiratory and end-expiratory volumes of each compartment was calculated as the VT. The OEP calculates absolute volumes. The absolute volume of each compartment at functional residual capacity (FRC) in control conditions was considered as the reference volume. Volumes are reported either as absolute values or as changes from the volume at FRC in control conditions. The total chest wall volume (Vcw) was modeled as the sum of volume of the upper rib cage, i.e., the rib cage apposed to the lung (Vrc,p), volume of the lower rib cage, i.e., the rib cage apposed to the abdomen (Vrc,a) and volume of the abdomen (Vab). Thus, the Vcw was calculated as $V_{cw} = V_{rc,p} + V_{rc,a} + V_{ab}$ and changes (Δ) in Vcw were calculated as $\Delta V_{cw} = \Delta V_{rc,p} + \Delta V_{rc,a} + \Delta V_{ab}$. The time course of the volume of each region (Vrc,p, Vrc,a and Vab) along their sum (Vcw) was processed to obtain a breath-by-breath assessment of both ventilatory pattern and operational chest wall volume. From VT and respiratory frequency, VE was calculated. VT was simultaneously measured by using a mass flow sensor (sVT). The volume accuracy of the OEP system was tested by comparing VToep to sVT. All respiratory cycles at rest and during walking were pooled for each subject.

The time course of the volume of each region (Vrc,p, Vrc,a and Vab) and their sum (Vcw) was processed to obtain a breath-by-breath assessment of both ventilatory pattern and operational chest wall volume (Johnson et al., 1999; Gorini et al., 1999).

3.2 Rib cage distortion measurements

a) The undistorted rib cage configuration was defined by plotting Vrc,p against Vrc,a during relaxation. Rib cage distortion was evaluated by comparing Vrc,p-Vrc,a at rest and during exercise to the undistorted rib cage configuration, according to the method of Chihara et al (1996). Thus we measured the perpendicular distance of the distorted configuration away from the relaxation line and divided it by the value of Vrc,p at the insertion point. This results in a dimensionless number, which, when multiplied by 100, gives percent distortion.

b) Because most patients were unable to relax their respiratory muscles enough to yield accurate and meaningful relaxation volume-pressure curves of the thorax, the presence of rib cage distortion was established by: 1. comparing the time courses of $V_{rc,p}$ vs $V_{rc,a}$ and 2. the phase shift between $V_{rc,a}$ and $V_{rc,p}$ when these two volumes were plotted against each other. This was measured as the ratio of distance delimited by the intercepts of $V_{rc,p}$ versus $V_{rc,a}$ dynamic loop on line parallel to the X-axis at 50% of RC_p tidal volume (m), divided by RC_a tidal volume (s), as $\theta = \sin^{-1} (m \cdot s^{-1})$, as previously adopted approach (Agostoni & Mognoni, 1996; Aliverti et al., 2009) (Fig. 5). In this system a phase angle of zero represents a completely synchronous movement of the compartments and 180° total asynchrony. Rib cage to abdomen displacement was assessed by the ratio of changes in V_{rc} to change in V_{ab} .

The rest signals were recorded over a 3-min period after a 10-min period of adaptation to equipment. In each patients, the volume tracings were normalized with respect to time to allow ensemble averaging over three reproducible consecutive breaths chosen within the period of interest (rest, warm-up, each minute of exercise) and to derive an average respiratory cycle over each of the data acquisition periods. Inspiratory and expiratory phases of the breathing cycles were derived from the V_{cw} signal.

3.3 Respiratory muscle pressure measurements

The pressure developed by inspiratory and expiratory rib cage muscles ($P_{rcm,i}$ and $P_{rcm,e}$, respectively) and that developed by the abdominal muscles (P_{abm}) were measured as the difference between the P_{es} - $V_{rc,p}$ loop and the relaxation pressure-volume curve of RC_p and between the P_{ga} - V_{ab} loops and the relaxation pressure-volume curve of the abdomen, respectively, according to the method of Aliverti et al. (1997).

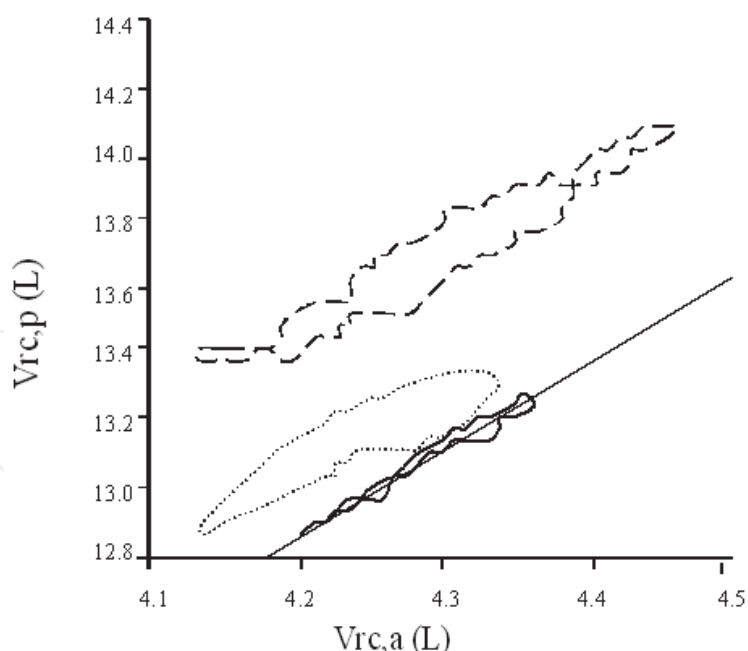


Fig. 4. The undistorted rib cage configuration is defined by plotting $V_{rc,p}$ against $V_{rc,a}$ during relaxation. Rib cage distortion is evaluated by comparing $V_{rc,p}$ - $V_{rc,a}$ at rest and during exercise to the undistorted rib cage configuration. Individual $V_{rc,p}$ - $V_{rc,a}$ plot at quiet breathing (QB) and at 50 L of VE. In a representative subject. Continuous lines: relaxation lines. Continuous loops: respiratory cycle at QB. Dotted loops: respiratory cycle during leg exercise; dashed loops: respiratory cycle during arm exercise.

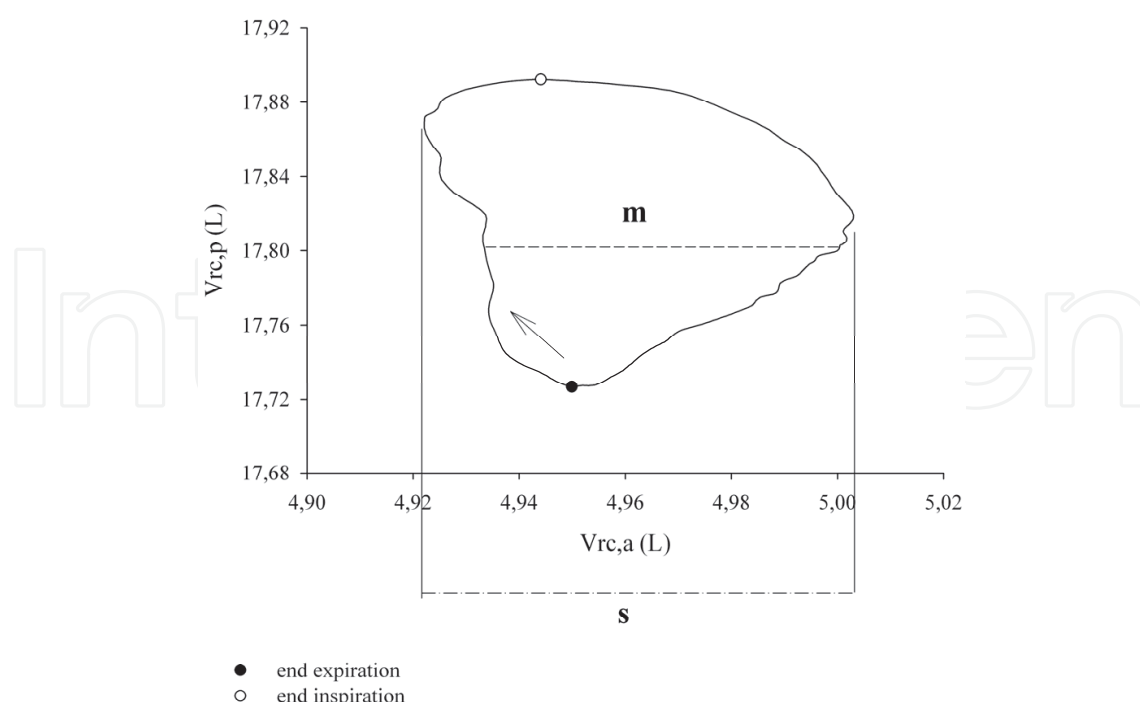


Fig. 5. In patients unable to relax their respiratory muscles enough to yield accurate and meaningful relaxation volume-pressure curves of the thorax, the presence of rib cage distortion is established by: 1. comparing the time courses of $V_{rc,p}$, $V_{rc,a}$ and 2. the phase shift between $V_{rc,a}$ and $V_{rc,p}$ when these two volumes are plotted against each other. This is measured as the ratio of distance delimited by the intercepts of $V_{rc,p}$, $V_{rc,a}$ dynamic loop on line parallel to the X-axis at 50% of RC_p tidal volume (m), divided by RC_a tidal volume (s), as $\theta = \sin^{-1} (m \cdot s^{-1})$. In this system a phase angle of zero represents a completely synchronous movement of the compartments and 180° total asynchrony.

4. Results and discussion

4.1 OEP vs pneumotachograph volume

We compared change in V_{cw} during inspiration obtained by OEP (ΔV_{cw}) with inspired volumes obtained by integration of flow (ΔV_m). Also, the linear regression analysis between ΔV_{cw} and ΔV_m calculated simultaneously over a period of 20s yielded the following equation: $r:0.94$, $Y = -0.103 + 1.093X$. The small discrepancy we found between V_{Toep} and V_{Tm} may be explained as follows. While pneumotachograph measures the volume of the lung OEP measures the volume of the trunk. This includes volume changes in the mouth, gas compression and decompression in the lung, and blood shift between trunk and extremity.

4.2 Physiology

4.2.1 Effect of exercise

Studies concerning chest wall mechanics during exercise or walking in normal humans (Kenyon et al., 1997; Aliverti et al., 1997; Sanna et al., 1999; Duranti et al., 2004) have used OEP to investigate a new aspect of respiratory mechanics: the rib cage distortion, that is due to the different pressure acting on the volumes of the lower (abdominal) and upper rib cage i.e., the non diaphragmatic inspiratory/expiratory muscles acting on volume of the upper

rib cage, and diaphragm and abdominal muscles acting on volume of the lower rib cage. The volume distortion surprisingly is $<1\%$ (Kenyon et al., 1997; Aliverti et al., 1997; Sanna et al., 1999). Thus, during exercise, the diaphragm, rib cage and abdominal muscles are coordinated so that rib cage distortion, although measurable, is minimised. In particular, the progressive relaxation of abdominal muscles observed during inspiration could prevent volume of the lower rib cage from an unbalanced expansion with respect to volume of the upper rib cage. (Aliverti et al., 1997; Sanna et al., 1999; Duranti et al., 2004)

4.2.2 Effect of coughing

The three-compartment model of the chest wall dictates that contraction of the abdominal muscles has both a deflationary action on the lower rib cage via their insertional components (the rectus and obliquus muscles), and an inflationary action via their non-insertional components (the transversus muscle), the net effect being that upper rib cage deflation is commensurate with lower rib cage deflation (Kenyon et al., 1999). However, if forces applied to the upper rib cage are out of proportion with those applied to the lower rib cage, distortion might ensue during fits of coughing. In this way the abdominal rib cage is exposed to greater positive abdominal pressure at the end of expiration during cough (Man et al., 2003). Lanini et al., (2007) therefore hypothesized that uneven distribution of operating forces may results in rib cage distortion during coughing. The results obtained in 12 healthy subjects during voluntary single and prolonged coughing efforts at functional residual capacity and after maximal inspiration (max) showed that the three chest wall compartments contributed to reducing end expiratory volumes of the chest wall during coughing at functional residual capacity and prolonged maximum coughing, with the latter resulting in the greatest chest wall deflation. Mean rib cage distortion, did not differ between men and women, but tended to significantly increase from single to prolonged coughing maximum. Lanini et al. (2007) therefore concluded that rib cage distortion may ensue during coughing, probably as a result of uneven distribution of forces applied to the rib cage.

4.3 Pathophysiology

4.3.1 Neuromuscular diseases (NMD)

NMD are characterized by progressive loss of muscle strength resulting in cough ineffectiveness with deleterious effects on the respiratory system (Bach, 1993; Bach, 1997). Assessment of cough effectiveness is therefore a prominent component of the clinical evaluation and respiratory care in these patients. Owing to uneven distribution of muscle weakness in neuromuscular patients (De Troyer & Estenne 1995). Lanini et al., (2008) hypothesized that forces acting on the chest wall may have impact on the compartmental distribution of gas volume resulting in a decrease in cough effectiveness. The current authors have shown that unlike controls patients were unable to reduce end expiratory chest wall volume and exhibited greater rib cage distortion during cough. Peak cough flow was negatively correlated with rib cage distortion, the greater the former the smaller the latter, but not with respiratory muscle strength. Therefore, insufficient deflation of chest wall compartments and marked rib cage distortion resulted in cough ineffectiveness in these neuromuscular patients.

4.3.2 Pathology of the rib cage

Few detailed physiological studies have been carried out in young pectus excavatum PE subjects either preoperatively or postoperatively (Mead et al., 1985); it has been suggested

however that the depression of the sternum limits the movement of the ribs especially in the lower ones, thus preventing the expansion of the lower thoracic cross-sectional area (Koumbourlis, 2009). On theoretical grounds uncoordinated displacement of chest wall compartments is not unexpected in these patients, considering that a non-uniform distribution of pressure over the different parts may distort the rib cage (Crawford et al., 1983; McCool et al., 1985; Chihara et al., 1996; Ward et al., 1992; Kenyon et al., 1997). By contrast, recent studies (Kenyon et al., 1997; Aliverti et al., 1997; Sanna et al., 1999; Romagnoli et al., 2006) have shown that the expiratory action of the abdominal muscles plays a key role in minimizing rib cage distortion during sustained ventilatory effort in healthy subjects. Moreover, a normal swing in abdominal pressure with a normal abdominal pressure-volume loop is associated with normal rib cage mobility during increased ventilation in PE patients (Mead et al., 1985). In keeping with these data, the preliminary results of our laboratory (Binazzi et al., 2009) indicate a normal reduction in end-expiratory abdominal volume (suggestive of phasic expiratory activity) during hyperventilation in PE patients. Collectively these data allow us to hypothesize that a coordinated motion of upper to lower rib cage prevents distortion during ventilatory tasks in PE patients. It has been suggested that the rib cage fails to move up and out during inspiration (Whol et al., 1995). Available data, however, argue against this possibility (Koumbourlis, 2009; Mead et al., 1985). Plotting of upper rib cage volume ($V_{rc,p}$) vs lower rib cage volume ($V_{rc,a}$) we were able to find a normal phase angle degree at QB and through maximal voluntary ventilation in control subjects and in a few PE patients.

4.3.3 Asthma

The mechanics of the chest wall was studied in asthmatic patients before and during histamine-induced bronchoconstriction. The volume of the chest wall (V_{cw}), pleural and gastric pressures were simultaneously recorded. V_{cw} was modeled as the sum of the volumes of the pulmonary-apposed rib cage ($V_{rc,p}$), diaphragm-apposed rib cage ($V_{rc,a}$), and abdomen (V_{ab}). During bronchoconstriction, hyperinflation was due to the increase in end-expiratory volume of the rib cage, whereas change in V_{ab} was inconsistent because of phasic recruitment of abdominal muscles during expiration. Changes in end-expiratory $V_{rc,p}$ and $V_{rc,a}$ were along the rib cage relaxation configuration, indicating that both compartments shared proportionally the hyperinflation. $V_{rc,p}$ - P_{pl} plot during bronchoconstriction was displaced leftward of the relaxation curve, suggesting persistent activity of rib cage inspiratory muscles throughout expiration. Changes in end-expiratory V_{cw} during bronchoconstriction did not relate to changes in airway obstruction or time and volume components of the breathing cycle. We concluded that during bronchoconstriction in asthmatic patients: (1) rib cage accounts largely for the volume of hyperinflation, whereas abdominal muscle recruitment during expiration limits the increase in V_{ab} ; (2) hyperinflation is influenced by sustained postinspiratory activity of the inspiratory muscles; (3) this pattern of respiratory muscle recruitment seems to minimize volume distortion of the rib cage at end-expiration and to preserve diaphragm length despite hyperinflation (Gorini et al., 1999).

4.3.4 Chronic obstructive pulmonary disease (COPD)

Lung hyperinflation in patients with chronic obstructive pulmonary disease (COPD) places the respiratory muscles at a mechanical disadvantage and impairs their force generation capacity (De Troyer, 1997). Clinical evidence of the diaphragm's vulnerability in the effect of

hyperinflation is abundant (Sharp, 1985). One indicator of diaphragm dysfunction is Hoover's sign (Hoover, 1920) consisting of inward movement of the lower lateral rib cage during inspiration. However, the basis of abnormal rib cage motion and the effect of hyperinflation on rib cage distortion have not been systematically examined in patients with COPD. Some factors argue against a close relationship between Hoover's sign and hyperinflation: (i) the primary factor contributing to rib cage distortion in COPD patients is an abnormal alteration of the forces applied to the pulmonary and abdominal rib cage, with hyperinflation making only a minor contribution (Jubran & Tobin, 1992); (ii) hyperinflation produces a decrease in airway resistance (Briscoe & Dubois, 1958) which may account for the greater degree of abnormal CW motion observed with resistive loading (Tobin et al., 1987) than with hyperinflation (Jubran & Tobin, 1992); (iii) hyperinflation is closely linked to expiratory flow limitation which at least theoretically, can be due entirely to loss of lung elastic recoil and tracheo or bronchomalacia. We therefore asked whether hyperinflation would produce rib cage distortion *per se*. We hypothesized that lung hyperinflation and rib cage distortion (Binazzi et al., 2008) could independently define the functional conditions of COPD patients. We based the hypothesis on the following observations: (i) a remarkable directed correlation has been found between abdominal rib cage compliance and distortability (Chihara et al., 1996), and (ii) passive tension in the abdominal muscles exerts an important deflationary action on abdominal rib during tidal inspiration (Kenyon et al., 1997). Rib cage distortion associated with Hoover's sign was indicated by the negative values of $V_{rc,p}/V_{rc,a}$ which contrasted with the positive values in patients without Hoover's sign. Most importantly, the fact that we found a lack of any significant relationship between quantitative indices of Hoover's sign and functional residual capacity validates the starting hypothesis that rib cage volume distortion cannot be fully explained by static hyperinflation in patients with COPD. Chihara et al. (1996) have also speculated that when rib cage distortion is present the greater the distortability the greater the degree of recruitment of inspiratory rib cage muscles and the greater the predisposition to dyspnea for a given load and strength (Ward & Macklem 1992). On the other hand, the role of hyperinflation on abnormal chest movement is questionable (Binazzi et al., 2008; Hoover, 1920; Aliverti et al., 2009; Jubran & Tobin, 1992; O'Donnell et al., 1997; O'Donnell et al., 2001). By contrast, Aliverti et al., (2009) have shown that lower rib cage paradox yields to an early onset of dynamic hyperinflation as a likely explanation for the increased dyspnea during incremental exercise in these patients. Contradicting this interpretation we have shown that, neither rib cage distortion nor, despite being reduced, dynamic lung hyperinflation do not contribute to oxygen-induced decrease in dyspnea in exercising normoxic COPD patients.

The coordinated respiratory muscle action translates into proportional changes in the volume of the CW compartments when human beings cycle, run or walk (Sanna et al., 1999; Aliverti et al., 1997; Duranti et al., 2004). This complex interaction between the diaphragm, inspiratory rib cage muscles, and abdominal muscles is poorly understood during unsupported arm exercise [UAE]. Comparing UAE with leg exercise [LE] in normal subjects Celli et al. (1988) found that UAE resulted in less ventilatory contribution of inspiratory muscles of the rib cage and more contribution by the diaphragm and abdominal muscles. In a two compartment rib cage model this shift in dynamic work results in rib cage distortion (Kenyon et al., 1997). Romagnoli et al., (2006) therefore hypothesized that a decrease in pressure contribution of the rib cage inspiratory muscles, and increase in pressure production of the diaphragm and abdominal muscles with UAE might be associated with

rib cage distortion as opposed to undistorted configuration during LE at comparable ventilation. The results showed that unlike LE, with UAE inspiratory pressure production of the rib cage muscles did not significantly increase from quiet breathing. However, no clear-cut differences in rib cage distortion were found between UAE and LE. What is the clinical relevance of this study? Based on the present results and those in patients with ankylosing spondylitis and rib cage rigidity (Romagnoli et al., 2004) we speculate that diverting rib cage muscles from ventilatory function to postural function limits inspiratory rib cage expansion more than some degree of rib cage rigidity does. This may have negative ventilatory consequences in severely hyperinflated patients with chronic obstructive pulmonary disease (COPD) who unlike the subjects of the present study are not able to deflate the rib cage and abdominal compartments to maintain an adequate tidal volume when using rib cage muscles for daily living activities.

4.3.5 Rib cage distortion and dyspnea

Both the joint and muscles receptors should sense the deformation of the chest wall occurring during hyperventilation and breathing through resistance. The information sent by these receptors could alter the pattern of activity of some respiratory muscles. Because of the phase shift between the change of lung volume and those of some parts of the rib cage there might be a phase shift between the different impulses from the lung receptors and the those of the rib cage. This paradoxical information contributes to a sensation of dyspnea (Agostoni & Mognoni, 1996). More recently Chihara et al., (1996) have speculated that when rib cage distortion is present the greater the distortability the greater the degree of recruitment of inspiratory rib cage muscles and the greater the predisposition to dyspnea for a given load and strength. However our recent data shown that BORG score on air did not differ between patients with and without rib cage distortion, and that changes in BORG with oxygen associated with no change in phase shift do not provide evidence that rib cage distortion plays a major role in the perceived sense of breathlessness. But that does not mean that it could not contribute as we do not have any evidence that phase shift accurately reflects the different pressures acting on lower and upper rib cage (Chihara et al., 1996; Kenyon et al., 1997), or energy wasted during inspiration on rib cage distortion. Further studies in these patients are needed to assess the relationship between changes in the applied muscle pressures, displacement of chest wall compartment, rib cage phase shift, and dyspnea during exercise, on air and oxygen.

Either dyspnea or leg effort, or both may be the principal complaints for stopping exercise in patients with COPD (O'Donnell et al., 1997; O'Donnell et al., 2001) Regardless of whether patients dynamically hyperinflated or deflated the chest wall, or distorted the rib cage, was dyspnea the primary symptom limiting exercise. These data are in keeping with those of Iandelli et al., (2002) who have found that externally imposed expiratory flow limitation does not necessarily lead to dynamic hyperinflation, nor to impaired exercise performance in subjects who do not hyperinflate the chest wall, and does not contribute to dyspnea in subjects who hyperinflate until the highest expiratory flow limitation exercise level is reached. Collectively these data are not in line with a previous report (Aliverti et al., 2009) showing that an early onset of dynamic hyperinflation of the chest wall is the most likely explanation of predominance of dyspnea in patients with rib cage distortion, and that when paradox is absent the sense of leg effort becomes a more important symptom limiting exercise. The effort-dependent nature of different exercise tests, underlying multifactorial mechanisms, and subjective nature of dyspnea scaling might account for these different

results. In conclusion, the rib cage paradox, changes in chest wall dimension and dyspnea do not appear to be closely interrelated phenomena during exercise in COPD patients.

4.3.6 Study limitations

The limitations of OEP in assessing the relative changes in $V_{rc,p}$ and $V_{rc,a}$ might be the changes in the cephalic margin of the zone of apposition, i.e., in the area over which the rib cage is effectively exposed to abdominal pressure (Chihara et al., 1996). Inasmuch as the area of apposition is diminished in patients with COPD, the abdominal rib cage is considerably smaller than normal. However, to the extent that abdominal displacement is the principal determinant of the upper boundary of the area of apposition (Kenyon et al., 1997), the similarity of this displacement at end inspiration during rest and exercise suggests that its caudal excursion during inspiration is not greatly affected by exercise. We therefore believe that an error, if any exists, introduced by defining the boundary of the upper limit of the area of apposition on the dynamics of abdominal rib cage and pulmonary rib cage would not qualitatively affect our results.

5. References

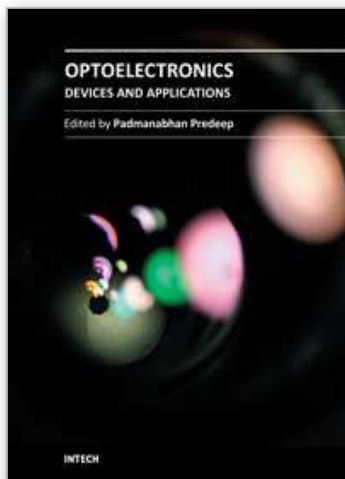
- Agostoni, E. & D'Angelo E. (1985). Statics of the chest wall. In: *The Thorax*, Editor, Roussos, Macklem, pp. 259-295, Publisher, Marcel Dekker, New York
- Jiang, TX. Demedts, M. & Decramer, M. (1988). Mechanical coupling of upper and lower canine rib cage and its functional significance. *Journal of Applied Physiology*, Vol. 64, pp. 620-626
- Ward, MEJW. & Macklem, PT. (1992). Analysis of human chest wall motion using a two compartment rib cage model. *Journal of Applied Physiology*, Vol.72, pp. 1338-1347
- Ringel, ER. Loring, SH. Mcfadden, ER. & Ingram, RH. (1983). Chest wall configurational changes before and during acute obstructive episodes in asthma. *American Review of Respiratory Disease*, Vol.128, pp. 607-610
- Urney, WF. Loring, SH. Mead, J. Brown, R. Slutsky, AS. Sarkarati, MS. & Rossier, A. (1981). Rib Cage (Rc) Mechanics In Quadriplegic Patients. *Physiologist*, Vol. 24, No. 4, pp. 97
- Crawford, ABH. Dodd, D. & Engel, LA. (1983). Changes in the rib cage shape during quiet breathing, hyperventilation and single inspiration. *Respiratory Physiology*, Vol 54, pp. 197-209
- McCool, FD. Loring, SH. & Mead J. (1985). Rib cage distortion during voluntary and involuntary breathing acts. *Journal of Applied Physiology*. Vol. 58, No5, pp. 1703-1712
- D'Angelo, E. (1981). Cranio-caudal rib cage distortion with increasing inspiratory airflow in man. *Respiratory Physiology*. Vol. 44 pp. 215-237
- Roussos, CS. Fixley, M. Geneset, J. Cosio, M. Kelly, S. Martin, RR. & Engel, LA. (1977). Voluntary factors influencing the distribution of inspired gas. *American Review of Respiratory Disease*. Vol. 116, pp. 457-467, ISSN
- Agostoni, E. & Mognoni, PJ. (1966). Deformation of the chest wall during breathing efforts. *Journal of Applied Physiology*. Vol. 21, No. 6, pp. 1827-1832.
- Sackner, MA. (1980). Monitoring of ventilation without a physical connection to the airway. In: *Diagnostic Techniques in Pulmonary Disease, Part I Volume 1*. pp. 508, Publisher: Marcel Dekker, New York.

- Gilbert, R. Auchincloss, JH. Brodsky, J. & Boden, W. (1972). Changes in tidal volume, frequency and ventilation induced by their measurement. *Journal of Applied Physiology*, Vol. 33, pp. 252-254
- Henke, KG. Sharratt, M. Pegelow, D. & Dempsey, JA. (1988). Regulation of end expiratory lung volume during exercise. *Journal of Applied Physiology*, Vol. 64, pp. 135-146
- Pedotti, A. & Ferrigno, G. (1995). Opto-electronics based systems. In *Three-Dimensional Analysis of Human Movement, Human Kinetics, 1st Ed*, Editors, Allard, P. Stokes, IA. Bianchi, J. pp. 57-78, Publishers, Human Kinetics. Champaign, USA.
- Cala, SJ. Kenyon, CM. Ferrigno, G. Carnevali, P. Aliverti, A. Pedotti, A. Macklem, P.T. & Rochester, DF. (1996). Chest wall and lung volume estimation by optical reflectance motion analysis. *Journal of Applied Physiology*, Vol. 81, pp.2680-2689
- Kenyon, CM. Cala, SJ. Yan, S. Aliverti, A. Scano, G. Duranti, R. Pedotti, A. & Macklem, P.T. (1997). Rib cage mechanics during quiet breathing and exercise in humans. *Journal of Applied Physiology*, Vol. 83, pp. 1242-1255
- Sanna, A. Bertoli, F. Misuri, G. Gigliotti, F. Iandelli, I. Mancini, M. Duranti, R. Ambrosino, N. & Scano, G. (1999). Chest wall kinematics and respiratory muscle action in walking healthy man. *Journal of Applied Physiology*, Vol. 87, pp. 938-946
- Aliverti, A. Cala, SJ. Duranti, R. Ferrigno, G. Kenyon, CM. Pedotti, A. Scano, G. Sliwinsky, P. Macklem, PT. & Yan, S. (1997). Human respiratory muscle actions and control during exercise. *Journal of Applied Physiology*, Vol. 83, pp.1256-1269
- Duranti, R. Sanna, A. Romagnoli, I. Nerini, M. Gigliotti, F. Ambrosino, N. & Scano, G. (2004). Walking modality affects respiratory muscle action and contribution to respiratory effort. *Pflugers Archives*, Vol.448, pp.222-230
- Romagnoli, I. Gigliotti, F. Lanini, B. Bianchi, R. Soldani, N. Nerini, M. Duranti, R. & Scano, G. (2004). Chest wall kinematics and respiratory muscle coordinated action during hypercapnia in healthy males. *European Journal of Applied Physiology*, Vol. 91, pp.525-533
- Romagnoli, I. Gigliotti, F. Galarducci, A. Lanini, B. Bianchi, R. Cammelli, D. & Scano, G. (2004) Chest wall kinematics and respiratory muscle action in ankylosing spondylitis patients. *European Respiratory Journal*, Vol. 24, pp. 453-460
- Romagnoli, I. Gorini, M. Gigliotti, F. Bianchi, R. Lanini, B. Grazzini, M. Stendardi, L. & Scano, G. (2006). Chest wall kinematics, respiratory muscle action and dyspnoea during arm vs. leg exercise in humans. *Acta Physiologica (Oxf)*, Vol. 188, pp. 63-73
- Binazzi, B. Lanini, B. Bianchi, R. Romagnoli, I. Nerini, M. Gigliotti, F. Duranti, R. Milic-Emili, J. & Scano, G. (2006). Breathing pattern and kinematics in normal subjects during speech, singing and loud whispering. *Acta Physiologica (Oxf)*, Vol. 186, pp. 233-246.
- Filippelli, M. Pellegrino, R. Iandelli, I. Misuri, G. Rodarte, J.R. Duranti, R. Brusasco, V. & Scano, G. (2001). Respiratory dynamics during laughter. *Journal of Applied Physiology*, Vol. 90, pp. 1441-1446
- Lanini, B. Bianchi, R. Binazzi, B. Romagnoli, I. Pala, F. Gigliotti, F. & Scano, G. (2007). Chest wall kinematics during cough in healthy subjects. *Acta Physiologica (Oxf)*, Vol. 190, pp. 351-358
- Gorini, M. Iandelli, I. Misuri, G. Bertoli, F. Filippelli, M. Mancini, M. Duranti, R. Gigliotti, F. & Scano, G. (1999). Chest wall hyperinflation during acute bronchoconstriction in asthma. *American Journal of Respiratory and Critical Care Medicine*, Vol. 160, pp. 808-816

- Filippelli, M. Duranti, R. Gigliotti, F. Bianchi, R. Grazzini, M. Stendardi, L. & Scano, G. (2003). Overall contribution of chest wall hyperinflation to breathlessness in asthma. *Chest*, Vol. 124, pp. 2164-2170
- Johnson, BD. Weisman, IM. Zeballos, RJ. & Beck, KC. (1999). Emerging concepts in evaluation of ventilatory limitation during exercise: the excessive tidal flow-volume loop. *Chest*, Vol. 116, pp. 488-503
- Chihara, K. Kenyon, CM. Macklem, PT. (1996). Human rib cage distortability. *Journal of Applied Physiology*. Vol. 81, No.1, pp. 437-447.
- Aliverti, A. Quaranta, M. Chakrabarti, B. Albuquerque, ALP. & Calverley, PM. (2009). Paradoxical movement of the lower ribcage at rest and during exercise in COPD patients. *European Respiratory Journal*, Vol. 33, pp. 49-60
- Man, WD. Kyrrousis, D. Fleming, TA. Chetta, A. Harraf, F. Mustfa, N. Rafferty, GF. Polkey, MI. & Moxham, J. (2003). Cough gastric pressure and maximum expiratory mouth pressure in humans. *American Journal of Respiratory and Critical Care Medicine*, Vol. 68, pp. 714-717
- Bach, JR. (1993). Mechanical insufflation-exsufflation: comparison of peak expiratory flows with manually assisted and unassisted coughing techniques. *Chest*, Vol. 104, pp. 1553-1562
- Bach, JR. Ishikawa, I. & Kim, H. (1997). Prevention of pulmonary morbidity for patients with Duchenne muscular dystrophy. *Chest*, Vol.112, pp. 1024-1028
- De Troyer, A. & Estenne, M. (1995). Respiratory system in neuromuscular disorders. In: *The Thorax Part C*, Editor, Roussos, C. pp. 2177-2212. Publisher, Marcel Dekker, New York, NY
- Lanini, B. Masolini, M. Bianchi, R. Binazzi, B. Romagnoli, I. Gigliotti, F. & Scano G. (2008). *Respiratory Physiology and Neurobiology*, Vol. 161, No. 1, pp. 62-68
- Mead, J. Sly, P. Le Souef, P. Hibbert, M. & Phelan, P. (1985). Rib cage mobility in Pectus Excavatum. *American Review of Respiratory Disease*. Vol. 132 pp.1223-1228
- Koumbourlis, C. (2009). Pectus excavatum: Pathophysiology and clinical characteristics. *Paediatric Respiratory Reviews*, Vol.10 pp. 3-6
- Binazzi, B. Coli, C. Innocenti Bruni, G. Gigliotti, F. Messineo, R. Lo Piccolo, R. Romagnoli, I. Lanini, B. & Scano, G. (2009). Breathing pattern and chest wall kinematics in patients affected by pectus excavatum. *European Respiratory Journal*, Vol. 34 No. 53
- Whol, ME. Stark, A. & Stokers, DC. (1995). Thoracic disorders in Childhood. In *The Thorax Part C, Disease*, Editor, Roussos, C. pp. 2035-2069. Publisher, Marcel Dekker New York, NY
- De Troyer, A. (1997). Effect of hyperinflation on the diaphragm. *European Respiratory Journal*, Vol.10, pp. 708-713
- Sharp, JT. (1985). The chest wall and respiratory muscles in airflow limitation. In: *The Thorax: Vital pump. Lung Biology in Healthy and Disease Series*, Editors, Macklem, PT. Roussos, C. & Lenfant, C. pp. 1155-1202, Publisher, Marcel Dekker, New York, NY
- Hoover, CF. (1920). The diagnostic significance of inspiratory movements of the costal margins. *American Journal. Medical Sciences*. Vol. 159, pp. 633-646
- Jubran, A. & Tobin, MJ. (1992). The effect of hyperinflation on rib cage-abdominal motion. *American Review of Respiratory Disease*, Vol. 146, pp. 1378-1382

- Briscoe,WA. & Dubois, AB. (1958). The relationship between airway resistance, airway conductance and lung volume in subjects of different age and body size. *Journal of Clinical Investigation*, Vol. 37, pp. 1279–1285
- Tobin, MJ. Perez, W. Guenther, SM. Lodato, RF. & Dantzker, DR. (1987). Does rib-cage abdominal paradox signify respiratory muscle fatigue? *Journal of Applied Physiology*, Vol. 63, pp. 851–860
- Binazzi, B. Bianchi, R. Romagnoli, I. Lanini, B. Stendardi, L. Gigliotti, F. & Scano G. (2008). Chest wall kinematics and Hoover's sign. *Respiratory Physiology and Neurobiology*, Vol. 160 No.3, pp. 325-333
- O'Donnell, DE. Bain, DJ. & Webb, K. (1997). Factors contributing to relief of exertional breathlessness during hyperoxia in chronic air flow limitation. *American Journal of Respiratory and Critical Care Medicine*, Vol.155 pp. 530-535
- O'Donnell, DE. D'arsigny, C. & Webb, K. (2001). Effects of hyperoxia on ventilatory limitation during exercise in advanced chronic obstructive pulmonary disease. *American Journal of Respiratory and Critical Care Medicine*, Vol. 163 pp. 892-898
- Celli, BR. Criner, G. & Rassulo, J. (1988). Ventilatory muscle recruitment during unsupported arm exercise in normal subjects. *Journal of Applied Physiology*, Vol. 54, pp. 1936-1941
- Iandelli, I. Aliverti, A. Kayser, B. Dellacà, R. Cala, SJ. Duranti, R. Kelly, S. Scano, G. Sliwinski, P. Yan, S. Macklem, PT. & Pedotti, A. (2002). Determinants of exercise performance in normal men with externally imposed expiratory flow limitation. *Journal of Applied Physiology*, Vol. 92, pp. 1943-1952

IntechOpen



Optoelectronics - Devices and Applications

Edited by Prof. P. Predeep

ISBN 978-953-307-576-1

Hard cover, 630 pages

Publisher InTech

Published online 03, October, 2011

Published in print edition October, 2011

Optoelectronics - Devices and Applications is the second part of an edited anthology on the multifaced areas of optoelectronics by a selected group of authors including promising novices to experts in the field. Photonics and optoelectronics are making an impact multiple times as the semiconductor revolution made on the quality of our life. In telecommunication, entertainment devices, computational techniques, clean energy harvesting, medical instrumentation, materials and device characterization and scores of other areas of R&D the science of optics and electronics get coupled by fine technology advances to make incredibly large strides. The technology of light has advanced to a stage where disciplines sans boundaries are finding it indispensable. New design concepts are fast emerging and being tested and applications developed in an unimaginable pace and speed. The wide spectrum of topics related to optoelectronics and photonics presented here is sure to make this collection of essays extremely useful to students and other stake holders in the field such as researchers and device designers.

How to reference

In order to correctly reference this scholarly work, feel free to copy and paste the following:

Giulia Innocenti Bruni, Francesco Gigliotti and Giorgio Scano (2011). Optoelectronic Plethysmography for Measuring Rib Cage Distortion, Optoelectronics - Devices and Applications, Prof. P. Predeep (Ed.), ISBN: 978-953-307-576-1, InTech, Available from: <http://www.intechopen.com/books/optoelectronics-devices-and-applications/optoelectronic-plethysmography-for-measuring-rib-cage-distortion>

INTECH
open science | open minds

InTech Europe

University Campus STeP Ri
Slavka Krautzeka 83/A
51000 Rijeka, Croatia
Phone: +385 (51) 770 447
Fax: +385 (51) 686 166
www.intechopen.com

InTech China

Unit 405, Office Block, Hotel Equatorial Shanghai
No.65, Yan An Road (West), Shanghai, 200040, China
中国上海市延安西路65号上海国际贵都大饭店办公楼405单元
Phone: +86-21-62489820
Fax: +86-21-62489821

© 2011 The Author(s). Licensee IntechOpen. This is an open access article distributed under the terms of the [Creative Commons Attribution 3.0 License](https://creativecommons.org/licenses/by/3.0/), which permits unrestricted use, distribution, and reproduction in any medium, provided the original work is properly cited.

IntechOpen

IntechOpen